

DOI: 10.1002/sml.200600061

## Inkjet Printing of Electrically Conductive Patterns of Carbon Nanotubes\*\*

Krisztián Kordás, Tero Mustonen, Géza Tóth, Heli Jantunen, Marja Lajunen, Caterina Soldano, Saikat Talapatra, Swastik Kar, Robert Vajtai,\* and Pulickel M. Ajayan

The advantageous physical properties of carbon nanotubes (CNTs), such as excellent thermal conductivity,<sup>[1]</sup> good mechanical strength,<sup>[2]</sup> optional semiconducting/metallic nature,<sup>[3]</sup> and advanced field-emission behavior,<sup>[4]</sup> have been utilized in a number of different devices for several years.<sup>[5]</sup> The area-selective synthesis of well-organized CNTs on pre-patterned growth templates using either catalytic<sup>[6]</sup> or plasma-enhanced<sup>[7]</sup> chemical vapor deposition methods (CCVD and PECVD, respectively) opens up further novel fields for advanced future applications. However, these promising techniques require complex lithography processes and sophisticated deposition facilities (PECVD) or are limited to thermally durable growth substrates (CCVD).

Recent advances in nanotube chemistry enable both the dissolution and dispersion of CNTs in various solvents.<sup>[8]</sup> These results suggest new alternatives for fabricating CNT patterns by simply dispensing/printing the dissolved/dispersed particles on substrates. Alternatively, controlled flocculation of CNT suspensions in flow channels or on prepat-

terned stamps can be accomplished to produce patterns of nanotubes on various surfaces.<sup>[9]</sup>

Herein, a cost-effective and scaleable deposition method for generating conductive multi-walled carbon nanotube (MWCNT) patterns on paper and polymer surfaces is presented. MWCNTs grown by CCVD were chemically modified to make the nanotubes dispersible in water, and in turn the aqueous dispersion was dispensed on various substrates using a commercial desktop inkjet printer. The electrical behavior of the printed patterns is investigated and the limitations of the process are discussed.

For functionalization (Figure 1a), the MWCNTs were first refluxed in nitric acid to produce carboxyl, hydroxyl, and carbonyl groups at the defect sites of the outer graphene layer of the nanotubes. In a subsequent step, these hydroxyl and carbonyl groups were oxidized further with potassium permanganate solution (in perchloric acid) to achieve additional carboxyl groups on the surfaces of the nanotubes.<sup>[10]</sup> Modifications of the as-grown CNT structure may be identified by comparison of the Raman spectra of the as-produced nanotubes (Figure 1b) and the fully functionalized nanotubes (Figure 1c) in the vicinity of the

[\*] Dr. R. Vajtai  
Rensselaer Nanotechnology Center  
Rensselaer Polytechnic Institute  
Troy, NY 12180 (USA)  
Fax: (+1) 518-2766540  
E-mail: vajtai@rpi.edu

Dr. K. Kordás, T. Mustonen, G. Tóth, Prof. H. Jantunen  
Microelectronics and Materials Physics Laboratories  
Department of Electrical and Information Engineering  
University of Oulu  
P.O. Box 4500, 90014 Oulu (Finland)

Prof. M. Lajunen  
Division of Organic Chemistry, Department of Chemistry  
University of Oulu  
P.O. Box 3000, 90014 Oulu (Finland)

C. Soldano  
Department of Physics, Applied Physics, and Astronomy  
Rensselaer Polytechnic Institute  
Troy, NY 12180 (USA)

Dr. S. Talapatra, Dr. S. Kar, Prof. P. M. Ajayan  
Department of Materials Science & Engineering  
Rensselaer Polytechnic Institute  
Troy, NY 12180 (USA)

[\*\*] The authors thank the Academy of Finland, the National Technology Agency of Finland (TEKES), the Graduate School of Infotech Oulu, the Tauno Tönnöngin Säätiö, and the Nokia Foundation for supporting this work. C.S., S.K., and P.M.A. acknowledge the support received from the Interconnect Focus Center New York at RPI.

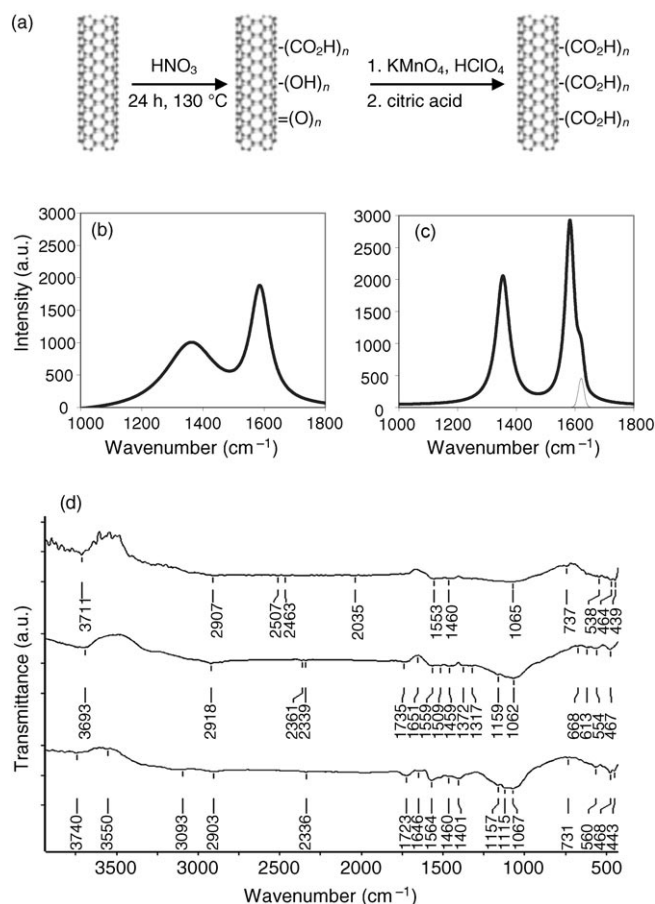


**Figure 1.** a) Schematic of MWCNT functionalization: refluxing in  $\text{HNO}_3$ , followed by treatment with  $\text{KMnO}_4$ . b, c) Raman spectra of the as-produced and functionalized nanotubes, respectively. d) Mid-IR spectra of MWCNTs: as-grown (top), treated in nitric acid (middle), and subsequently treated in  $\text{KMnO}_4/\text{HClO}_4$  solution (bottom).

D band ( $\approx 1350\text{ cm}^{-1}$ ) and G band ( $\approx 1582\text{ cm}^{-1}$ ) of graphite. Two distinct features can be clearly seen in the spectrum of the treated nanotubes. First, there is a marked increase in the D-band (relative) intensity, which can be attributed to the  $\text{sp}^3$  hybridization on the nanotubes due to oxygen functionalization. Second, the D' mode ( $\approx 1618\text{ cm}^{-1}$ ) appears due to the strained C=C vibration as a result of functionalization (a fitted peak is displayed in Figure 1c). Other typical signatures of functionalization, such as more defined second-order modes (not shown here), were also observed in the treated samples. The differences between as-grown, nitric acid treated, and consecutively potassium permanganate treated nanotubes are shown in greater detail by infrared spectroscopy (Figure 1d). Increased absorbance at wave numbers assigned to C–O stretching and out-of-plane deformations around  $1158\text{ cm}^{-1}$  and C=O stretching ( $1723\text{--}1735\text{ cm}^{-1}$ ) of the carboxyl groups are seen after the partial oxidation with nitric acid. However, when the nitric acid treatment is followed by further oxidation using potassium permanganate, increased absorbances for O–H bending ( $1401\text{ cm}^{-1}$ ) and C=O stretching ( $1723\text{--}1735\text{ cm}^{-1}$ ) of the carboxyl groups are found. C=C stretching in MWCNTs ( $1553\text{--}1564\text{ cm}^{-1}$ ) is also seen in the spectra, as has been reported by several research groups.<sup>[11]</sup> The position of the C=O stretch is changed, and the band intensity is reduced due to the heterogeneous environment at the surface of MWCNTs.<sup>[12]</sup>

Printable inks of the functionalized nanotubes were obtained by sonicating MWNT-(CO<sub>2</sub>H)<sub>n</sub> (10 mg) in water (10 mL) for 0.5 h. After sonication, the solution was stirred vigorously for 24 h and then centrifuged at 4000 rpm for 15 min. The supernatant solution was collected and centrifuged again. The procedure was repeated until a stable, homogeneous dispersion was achieved (typically four times). The as-made dark gray but transparent dispersion having a MWNT-(CO<sub>2</sub>H)<sub>n</sub> concentration of  $\approx 0.26\text{ mg mL}^{-1}$  proved to be stable over several days of storage. Field-emission scanning electron microscopy (FESEM) revealed that, in the course of the chemical modification, the length of the nanotubes became considerably shorter ( $1\text{--}5\text{ }\mu\text{m}$ ) as compared to that of the starting materials ( $1\text{--}2\text{ mm}$ ). The obtained ink was loaded into a cleaned printer cartridge and printed on transparency foil and paper (Figure 2). As the dispensed ink dried, the nanotubes formed tangled, randomly oriented networks on the surfaces. Electrically conductive CNT patterns could be achieved only by multiple prints over the same pattern (minimum of 30 repetitions for both substrates). As expected, the conductivity of the patterns increased with the number of print repetitions (Figure 3) because of the better percolation of the deposited CNTs.

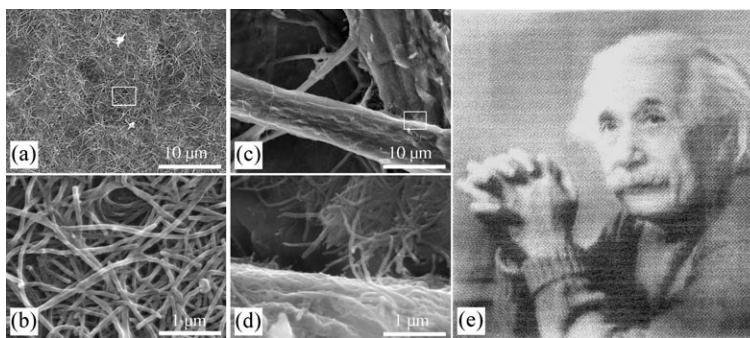


**Figure 2.** Multiple prints ( $\times 90$ ) of carboxylated MWCNTs on a, b) Canon BT-400 plastic and c, d)  $80\text{ g m}^{-2}$  paper surfaces. e) Scanned image of a photograph ( $105\text{ mm} \times 110\text{ mm}$ ) printed ( $\times 5$ ) on Xerox color copier paper ( $100\text{ g m}^{-2}$ ) using the water-based CNT ink.

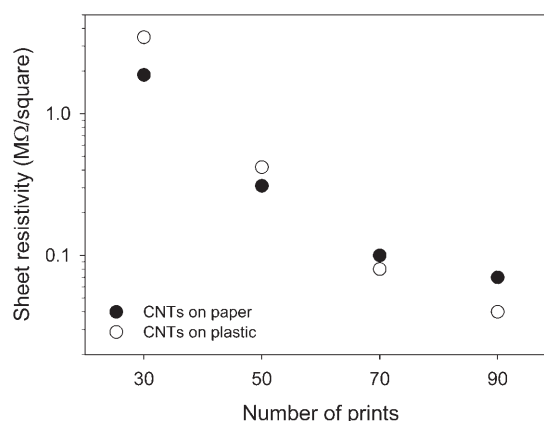


**Figure 3.** Sheet resistivity of the CNT patterns printed on paper and transparency foil as a function of print repetition (CNT coverage).

The measured impedance and phase dispersion curves (Figure 4) show typical parallel resistance/inductance/capacitance (RLC) circuit behavior. Depending on the density of

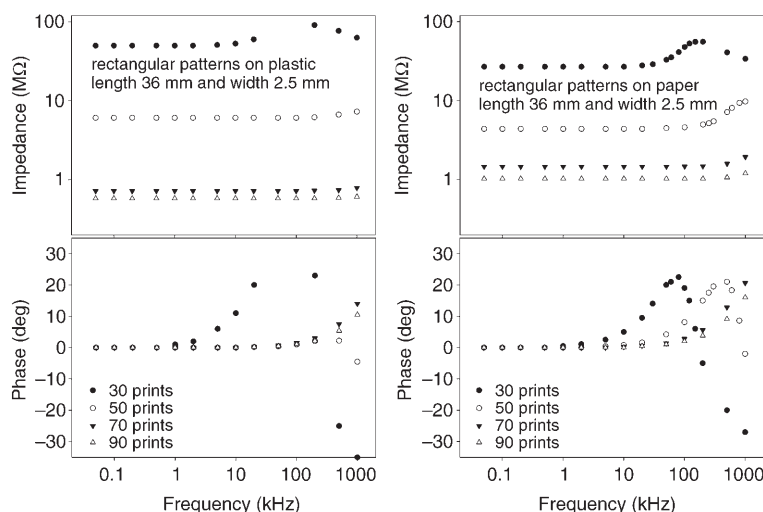


**Figure 4.** Impedance ( $Z$ ) and phase ( $\phi$ ) dependence on the frequency ( $f$ ,  $0.05\text{--}1000\text{ kHz}$ ) as measured for lines of CNTs  $36\text{-mm}$  long and  $\approx 2.5\text{-mm}$  wide printed on plastic and paper surfaces. The printed patterns were equipped with sputtered platinum contact pads ( $\approx 50\text{ nm}$  in thickness).

the deposited tangled CNT networks, the structures show ohmic conductance ( $\phi \approx 0^\circ$ ) up to a few kilohertz (lower density) or a few tens of kilohertz (higher density), whereas at higher frequencies the inductive and capacitive components determine the charge transport. The inductive behavior is explained by the curved nanotubes, which can be considered as tiny coils being randomly oriented and connected on the surface. For low nanotube densities, such coils act as individual components, that is, the local magnetic fields caused by the particular coils do not affect each other. In contrast, when the nanotube density is high, due to the proximity of the randomly oriented curved nanotubes, the sum of the inductance is decreased. For geometric reasons the inductance is more pronounced on paper than on plastic surfaces, since the deposited nanotubes wrap around the microscopic paper fibers causing a decreased radius of curvature for the microcoils of CNTs on the surface. As the frequency is increased, the capacitive coupling between the CNTs takes over the parallel inductance, thus decreasing the total impedance. From simple geometrical considerations for nanotubes of various densities on the surface, the total capacitive impedance must remain fairly constant. Therefore, the shift of impedance resonance toward the higher frequencies with an increased print number explains well the vanishing inductive transport for the CNT deposits of higher surface density. For a full understanding of the effects behind the high inductance values one needs to take into account nano- and mesoscopic scale effects along with the above-mentioned microscopic equivalents of macroscale properties.

Measurement of dc current–voltage curves ( $-10$  to  $+10$  V) for the printed lines showed linear behavior for each sample. However, the resistance values of the printed patterns varied as the ambient air quality changed in the course of data acquisition. It is known that the carrier concentration in the outer graphene layer of MWCNTs—which is responsible for electrical transport—changes when molecules are adsorbed on the surface. This effect has been exploited in gas sensor applications.<sup>[13]</sup> Our printed samples showed sensitivity to the vapor of several chemical substances, such as water, ammonia, and methanol, but remained inert to ethanol and 2-propanol (Table 1).

Droplets ( $0.5 \mu\text{L}$  each) of the CNT ink were dispensed manually onto the substrates with a transfer pipette to investigate surface wetting and morphology after drying. On transparency foil, our ink showed good wetting of the surface. When the water evaporated, most of the nanotubes were left behind at the perimeter of the original footprint,

and formed a ring-shaped CNT pattern. In the case of the hydrophobic paper surface, the ink droplet did not spread. As the solvent evaporated, the nanotubes formed a circle-shaped deposit with fairly uniform contiguous surface coverage. The deposits are randomly oriented on both substrates (Figure 5).

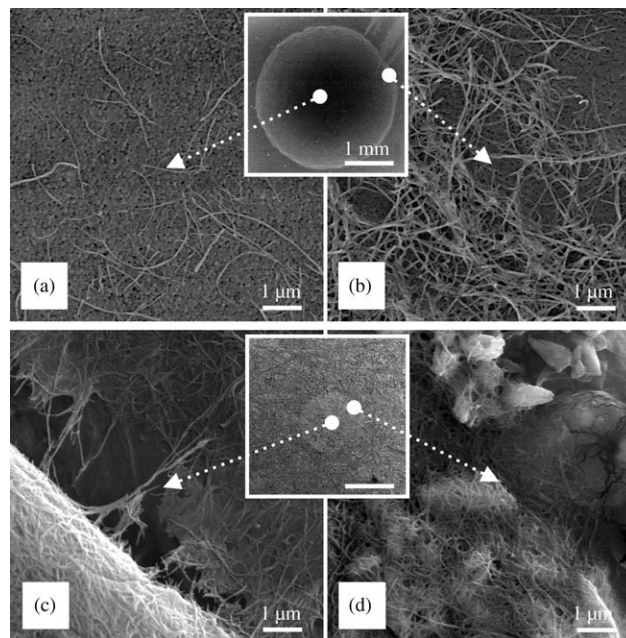


**Figure 5.** FESEM images of dried droplets of ink deposited with a micropipette ( $0.5 \mu\text{L}$  each). a) Center and b) perimeter of the residual ring-shaped pattern on transparency foil shown in the upper inset. c) Center and d) perimeter of a uniform CNT “disk” on paper shown in the lower inset.

In conclusion, a simple method for generating electrically conductive CNT patterns on paper and plastic surfaces has been demonstrated. MWCNTs grown by CCVD were carboxylated and dispersed in water to prepare nanotube dispersions, which are suitable for inkjet printing. By applying multiple prints, patterns having a sheet resistivity of  $\approx 40 \text{ k}\Omega/\square$  could be achieved. A great advantage of our process is that the printed patterns do not require curing, which is known to be a limiting factor for conventional conductive ink applications. Since our ink is a simple aqueous dispersion of functionalized nanotubes, it is environmentally friendly (see Note in the Experimental Section), easy to handle and store, and also enables the use of inexpensive printing cartridges and substrates. This method might find applications in rapid prototyping of resistive components, electromagnetic interference shielding, and gas sensors. It is assumed that with proper optimization of the printing parameters, such as improved substrate-alignment accuracy and ink rheology, and increased nanotube concentration, the method will become a mature and competitive technology for fabricating future low-cost CNT devices, for example, porous electrodes, flexible displays, and radio-frequency/microwave components.

**Table 1.** Relative resistance change  $\Delta R/R_0$  of the CNT patterns printed on paper. The pressure values correspond to the saturated vapor pressure of each substance at 295 K.

Substance	Vapor pressure [mm Hg]	$\Delta R/R_0$
water	17	$\approx 1.0$
ammonia	580	$\approx 1.5$
methanol	128	$\approx 0.5$
ethanol	50	$< 0.1$
2-propanol	44	$< 0.1$

## Experimental Section

MWCNTs with lengths of 1–2 mm and a tube diameter of 10–70 nm were grown on Si/SiO<sub>2</sub> wafers ( $\approx 1\text{-}\mu\text{m}$  thermal oxide) by the CCVD method in a continuous tube reactor at 770 °C. A solution of ferrocene (10 g) in xylene (1 L) was fed at a rate of 0.1 mL min<sup>-1</sup> into an evaporator column preheated to 185 °C, from which the vapor of ferrocene and xylene was introduced into the reactor using argon as carrier gas (30 cm<sup>3</sup> min<sup>-1</sup>, 1 atm). Growth periods of up to 2.5 h were applied. The synthesized mats of aligned MWCNTs were detached from the templates by dissolving the SiO<sub>2</sub> surface in hydrofluoric acid/ethanol (3:7 v/v). The freestanding mats were thoroughly flushed in ethanol and dried with pressurized nitrogen.

A typical procedure for carboxylation was as follows. MWCNTs (20 mg) were sonicated for 10 min and then refluxed in concentrated HNO<sub>3</sub> (20 mL) for 24 h. After cooling, the acidic solution was poured into deionized water (200 mL), filtered with coarse filter paper, and the residue was washed with deionized water until pH  $\approx 7$  was reached and finally dried at 120 °C for 4 h. The mass of the product ( $\approx 15$  mg) was somewhat lower than that of the raw material ( $\approx 20$  mg) because of the removed amorphous carbon and iron catalyst. To complete the oxidation of hydroxyl and carbonyl groups, the samples were sonicated in deionized water (10 mL), and KMnO<sub>4</sub> solution (45 mg KMnO<sub>4</sub> in 10.5 mL 70% HClO<sub>4</sub>) was added. After 10 min of vigorous stirring, citric acid solution (0.0148 M, 21 mL) was added to quench the KMnO<sub>4</sub>. Finally, the product of carboxylated nanotubes, MWCNT-(CO<sub>2</sub>H)<sub>n</sub>, was isolated by filtration and washed with water. Raman spectroscopy measurements were performed using a Renishaw Raman microscope, with the 514.5-nm line from an argon-ion laser operating at a power of 24 mW, and a Zeiss microscope with a 50 $\times$  objective. The Raman spectra were acquired from different positions in the samples to verify the repeatability and consistency of the data. Six accumulations for each position, with an accumulation time of 10 s, were maintained for the Raman measurements shown.

A desktop bubble-jet printer (Canon BJC 4550) was used for printing the nanotube patterns on commercial office paper (paper, 80 gm<sup>-2</sup>) and transparency foil (Canon BT-400). For single printouts, the resolution of printing with our nanotube ink was at least as good as that with a commercial black dye (Canon BC 20 BJ). As a result of the high surface tension of our water-based CNT ink, the dispensed droplets did not spread on the surfaces as much as ink containing ordinary dye. The narrowest lines we were able to print had a width of  $\approx 70$   $\mu\text{m}$ , which corresponded to a printing resolution of  $\approx 360$  dpi (dots per inch). However, with multiple printing such a high resolution could not be achieved due to the inaccuracy of the paper feeding mechanism. The typical tolerance for the lateral paper positioning was  $\pm 200$   $\mu\text{m}$  for both paper and transparency sheets.

To ensure good electrical contact with the deposited nanotubes, thin ( $\approx 50$  nm) contact pads (3 mm in diameter) of Pt were sputtered on the samples through a shadow mask. In the course of the  $Z$ - $f$  and  $\phi$ - $f$  analyses, the electrical probing and measurements were carried out using micromanipulators (Wentworth) connected to a precision RLC meter (HP 4284A equipped with a 16047A test fixture). For the four-point  $I$ - $V$  measurements of the sensor structures, the printed nanotubes were equipped

with thin ( $\approx 50$  nm) rectangular fingers of evaporated Pd electrodes. A commercial Ag paste was used to ensure good contact with the terminals of a source meter (Keithley 6434). The effect of resistive heating due to the probe current could be neglected since the maximum joule heat dissipated during the measurements was less than 1 mW.

Note: The toxicological effects of our nanotube ink need future investigation. However, because there are no additives such as surfactants and other volatile organic compounds—unlike in commercial inks—the only toxicological effect may arise from the nanotubes themselves. The toxicological effects of CNTs are disputed and are being investigated.<sup>[14]</sup> The inflammatory effects of CNTs are mostly due to residual catalyst particles, most of which are removed during the first oxidation step of our process (i.e., in the course of the nitric acid treatment). The respiratory toxicity of CNTs, if there is any, is not significant when the nanotubes are printed on paper. We rubbed the MWCNT printouts strongly with an eraser and found no considerable vanishing of the printed patterns. The tangling of nanotubes with paper fibers, as well as the hydrogen bonding of carboxyl-functionalized nanotubes with cellulose molecules, could prevent the CNTs detaching from the surface; thus, any respiratory exposure to CNTs is expected to be insignificant.

## Keywords:

carbon nanotubes • chemical vapor deposition • inkjet printing • oxidation • patterning

- 
- [1] a) S. Berber, Y. K. Kwon, D. Tomanek, *Phys. Rev. Lett.* **2000**, *84*, 4613; b) J. W. Che, T. Cagin, W. A. Goddard, *Nanotechnology* **2000**, *11*, 65; c) R. S. Ruoff, D. C. Lorents, *Carbon* **1995**, *33*, 925.
- [2] a) H. E. Troiani, M. Miki-Yoshida, G. A. Camacho-Bragado, M. A. L. Marques, A. Rubio, J. A. Ascencio, M. Jose-Yacamán, *Nano Lett.* **2003**, *3*, 751; b) M. Sammalkorpi, A. Krashenninnikov, A. Kuronen, K. Nordlund, K. Kaski, *Phys. Rev. B* **2004**, *70*, 245416; c) A. Y. Cao, V. P. Veedu, X. S. Li, Z. L. Yao, M. N. Ghosemi-Nejhad, P. M. Ajayan, *Nat. Mater.* **2005**, *4*, 540;
- [3] a) S. Li, Z. Yu, C. Rutherglen, P. J. Burke, *Nano Lett.* **2004**, *4*, 2003; b) G. Gruner, *Proc. SPIE Int. Soc. Opt. Eng.* **2005**, *5592*, 175; c) W. Hoenlein, F. Kreupl, G. S. Duesberg, A. P. Graham, M. Liebau, R. Seidel, E. Unger, *AIP Conf. Proc.* **2004**, *723*, 565; d) L. B. Kish, P. M. Ajayan, *Appl. Phys. Lett.* **2005**, *86*, 093106; e) J. E. Fischer, H. Dai, A. Thess, R. Lee, N. M. Hanjani, D. L. Dehaas, R. E. Smalley, *Phys. Rev. B* **1997**, *55*, R4921; f) B. Xiang, Y. Zhang, T. H. Wang, J. Xu, D. P. Yu, *Mater. Lett.* **2006**, *60*, 754; g) A. P. Graham, G. S. Duesberg, R. V. Seidel, M. Liebau, E. Unger, W. Pamler, F. Kreupl, W. Hoenlein, *Small* **2005**, *1*, 382.
- [4] a) J. T. H. Tsai, H. C. Ko, *Appl. Phys. Lett.* **2006**, *88*, 013104; b) W. A. Deheer, A. Chatelain, D. Ugarte, *Science* **1995**, *270*, 1179.
- [5] a) A. Modi, N. Koratkar, E. Lass, B. Q. Wei, P. M. Ajayan, *Nature* **2003**, *424*, 171; b) H. Dai, *Acc. Chem. Res.* **2002**, *35*, 1035; c) S. Chopra, K. McGuire, N. Gothard, A. M. Rao, A. Pham, *Appl. Phys. Lett.* **2003**, *83*, 2280; d) M. Terrones, A. Jorio, M. Endo, A. M. Rao, Y. A. Kim, T. Hayashi, H. Terrones, J.-C. Charlier, G. Dresselhaus, M. S. Dresselhaus, *Mater. Today* **2004**, *7*, 30.
- [6] a) K. Hernadi, Z. Konya, A. Siska, J. Kiss, A. Oszko, J. B. Nagy, I. Kiricsi, *Mater. Chem. Phys.* **2003**, *77*, 536; b) Y. J. Jung, B. Q. Wei, R. Vaitai, P. M. Ajayan, Y. Homma, K. Prabhakaran, T. Ogino,

- Nano Lett.* **2003**, *3*, 561; c) B. Q. Wei, R. Vajtai, Y. Jung, J. Ward, R. Zhang, G. Ramanath, P. M. Ajayan, *Nature* **2002**, *416*, 495.
- [7] a) R. Krishnan, H. Q. Nguyen, C. V. Thompson, W. K. Choi, Y. L. Foo, *Nanotechnology* **2005**, *16*, 841; b) Q. Zhang, S. F. Yoon, J. Ahn, B. Gan, Rusli, M. B. Yu, *J. Phys. Chem. Solids* **2000**, *61*, 1179.
- [8] a) K. Niesz, I. Vesselenyi, D. Mehn, Z. Konya, I. Kiricsi, *Mater. Sci. Forum* **2005**, *473–474*, 141; b) Y. J. Kim, Y. A. Kim, T. Chino, H. Suezaki, M. Endo, M. S. Dresselhaus, *Small* **2006**, *2*, 339; c) L. Marty, A.-M. Bonnot, A. Bonhomme, A. Iaia, C. Naud, E. André, V. Bouchiat, *Small* **2006**, *2*, 110; d) C. Kocabas, S.-H. Hur, A. Gaur, M. A. Meitl, M. Shim, J. A. Rogers, *Small* **2005**, *1*, 1110; e) D. Nepal, K. E. Geckler, *Small* **2006**, *2*, 406; f) Y.-P. Sun, K. Fu, Y. Lin, W. Huang, *Acc. Chem. Res.* **2002**, *35*, 1096; g) H. Kuzmany, A. Kukovecz, F. Simon, A. Holzweber, C. Kramberger, T. Pichler, *Synth. Met.* **2004**, *141*, 113; h) X. Zhang, T. V. Sreekumar, T. Liu, S. Kumar, *J. Phys. Chem. B* **2004**, *108*, 16435; i) M. S. Raghuvier, A. Kumar, M. J. Frederick, G. P. Louie, P. G. Ganesan, G. Ramanath, *Adv. Mater.* **2006**, *18*, 547; j) K. Balasubramanian, M. Burghard, *Small*, **2005**, *1*, 180.
- [9] a) Z. Fan, T. Wei, G. Luo, F. Wei, *J. Mater. Sci.* **2005**, *40*, 5075; b) J.-U. Park, M. A. Meitl, S.-H. Hur, M. L. Usrey, M. S. Strano, P. J. A. Kenis, J. A. Rogers, *Angew. Chem.* **2006**, *118*, 595; *Angew. Chem. Int. Ed.* **2006**, *45*, 581; c) M. A. Meitl, Y. Zhou, A. Gaur, S. Jeon, M. L. Usrey, M. S. Strano, J. A. Rogers, *Nano. Lett.* **2004**, *4*, 1643.
- [10] a) M. Burghard, V. Krstic, G. Duesberg, G. Philipp, J. Muster, S. Roth, *Synth. Met.* **1999**, *103*, 2540; b) T. Sainsbury, D. Fitzmaurice, *Chem. Mater.* **2004**, *16*, 2174.
- [11] a) J. Chen, M. A. Hamon, H. Hu, Y. Chen, A. M. Rao, P. C. Eklund, R. C. Haddon, *Science* **1998**, *282*, 95; b) Y. Qin, L. Liu, J. Shi, W. Wu, J. Zhang, Z. Guo, Y. Li, D. Zhu, *Chem. Mater.* **2003**, *15*, 3256.
- [12] T. Sainsbury, J. Stolarczyk, D. Fitzmaurice, *J. Phys. Chem. B* **2005**, *109*, 16310.
- [13] a) O. K. Varghese, P. D. Kichambre, D. Gong, K. G. Ong, E. C. Dickey, C. A. Grimes, *Sens. Actuators B* **2001**, *81*, 32; b) C. Cantalini, L. Valentini, L. Lozzi, I. Armentano, J. M. Kenny, S. Santucci, *Sens. Actuators B* **2003**, *93*, 333; c) E. Bekyarova, M. Davis, T. Burch, M. E. Itkis, B. Zhao, S. Sunshine, R. C. Haddon, *J. Phys. Chem. B* **2004**, *108*, 19717; d) C. Staii, A. T. Johnson, Jr., *Nano Lett.* **2005**, *5*, 1774.
- [14] a) S. K. Smart, A. I. Cassidy, G. Q. Lu, D. J. Martin, *Carbon* **2006**, *44*, 1034; b) S. Fiorito, A. Serafino, F. Andreola, P. Bernier, *Carbon* **2006**, *44*, 1100; c) J. Muller, F. Huaux, D. Lison, *Carbon* **2006**, *44*, 1048.

Received: February 3, 2006